

www.acsami.org Research Article

Emulsion Assembly of Graphene Oxide/Polymer Composite Membranes

Quynh P. Ngo, Weize Yuan, You-Chi Mason Wu, and Timothy M. Swager*



Cite This: ACS Appl. Mater. Interfaces 2023, 15, 21384-21393



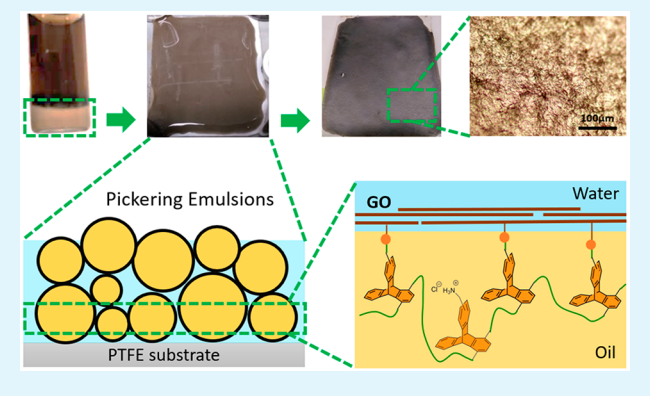
ACCESS I

III Metrics & More

Article Recommendations

Supporting Information

ABSTRACT: Graphene oxide/polymer composite water filtration membranes were developed via coalescence of graphene oxide (GO) stabilized Pickering emulsions around a porosity-generating polymer. Triptycene poly(ether ether sulfone)-CH₂NH₂:HCl polymer interacts with the GO at the water—oil interface, resulting in stable Pickering emulsions. When they are deposited and dried on polytetrafluoroethylene substrate, the emulsions fuse to form a continuous GO/polymer composite membrane. X-ray diffraction and scanning electron microscopy demonstrate that the intersheet spacing and thickness of the membranes increased with increasing polymer concentration, confirming the polymer as the spacer between the GO sheets. The water filtration capability of the composite membranes was tested by removing Rose Bengal from water, mimicking separations of weak black liquor waste. The composite membrane



achieved 65% rejection and 2500 g m⁻² h⁻¹ bar⁻¹. With high polymer and GO loading, composite membranes give superior rejection and permeance performance when compared with a GO membrane. This methodology for fabrication membranes via GO/polymer Pickering emulsions produces membranes with a homogeneous morphology and robust chemical separation strength.

KEYWORDS: Pickering emulsions, graphene oxide composite membranes, water—oil interface, porous polymer, graphene oxide, water filtration membranes, poly(ether ether sulfone), coalescence, polytetrafluoroethylene

■ INTRODUCTION

Thermal-based chemical separation methods such as evaporation, distillation, and drying are very costly in terms of energy and resources, and alternative membrane-based separations can reduce the energy consumption in these processes by 90%. Graphenes have been identified as excellent materials to produce water filtration membranes as a result of their laminar structure and their ability to introduce tunable physicochemical characteristics. Graphene oxide (GO) is a disordered material with functional groups including hydroxyl (OH), alkoxy (COC), carbonyl (CO), and carboxylic acid (COOH) species connected to the surfaces and at edges. These functional groups significantly increase the water solubility and reactivity.3 However, the mechanical integrity of GO membranes under high pressure in water filtration is limited, as it relies on the hydrophobic or π - π interactions between the GO sheets, and stronger interactions are needed to improve strength. Combining GO with polymers has been identified as an attractive approach because the composite membranes can have improved mechanical strength and high water permeability and preserve the attractive structural features of a GO membrane. 5-8

The current fabrication of GO/polymer composites includes flow-directed filtration, 9 film coating, 10,11 and layer-by-layer

assembly, ¹² and these methods require complicated multistep processes and suffer from GO aggregation. GO is generally dispersed in water, which in previous studies requires pairing with a water-soluble polymer. ¹² However, GO can undergo uncontrolled aggregation with polymers in water, ¹³ which creates challenges for the formation of homogeneous membranes. Methods separating polymer solutions and GO dispersions such as layer-by-layer deposition can circumvent the aggregation, but these processes are slow and require controlled conditions. ¹⁴

In previous work, we showed the chemical reaction of functionalized carbon nanotubes with primary amines at the interfaces of Pickering oil-in-water emulsions. In a related method, we now report Pickering oil-in-water and water-in-oil emulsions stabilized by GO, which has intrinsic reactivity with primary amines. As a result of the polar and nonpolar characteristics of GO sheets, these Pickering emulsions present

Received: February 23, 2023 Accepted: April 6, 2023 Published: April 18, 2023





Scheme 1. Synthesis of TripPEES-CH2NH2:HCl

nanomembrane structures at their interfaces. Spreading of viscous emulsions leads to the formation of a homogeneous GO/polymer membrane with polymer spacers cross-linking GO sheets. In contrast to other methods, polymers with poor water solubility can be used, thereby expanding the design space.

■ RESULTS AND DISCUSSION

As detailed in Scheme 1, we synthesized a porosity-generating polymer, triptycene poly(ether ether sulfone)-CH₂NH₂:HCl (TripPEES-CH₂NH₂:HCl), with pendant primary amines for cross-linking with GO. We chose to incorporate triptycene in the polymer chain because of its three-dimensional rigid structure, which has been widely used as a structural motif to create porous organic materials.²⁰ Porosity increases the membrane permeability,²¹ and the PEES backbone is chosen based on its excellent mechanical properties.²²

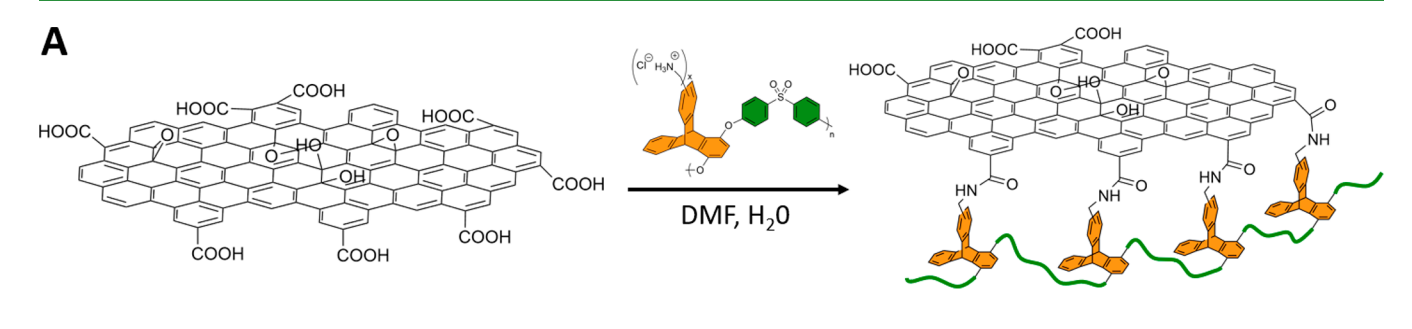
The TripPEES synthesis (Scheme 1) was adapted from a previous report, ²³ and full details of the synthesis can be found in Methods. To obtain the final product, TripPEES is chloromethylated to make TripPEES-CH₂Cl and a Gabriel primary amine synthesis produces TripPEES-CH₂NH₂. To increase the solubility in organic solvents, the HCl salt derivative of the polymer is prepared.

After obtaining TripPEES-CH2NH2:HCl polymer, we used FT-IR to determine its interaction with GO (Figure 1). The reaction was conducted in a homogeneous solution by mixing a 0.06 wt % polymer solution in dimethylformamide (DMF) and a 0.4 wt % GO aqueous dispersion. The product was dried, and the FT-IR spectra were taken. Figure 1B shows the FT-IR spectra of GO (blue), TripPEES-CH2NH2:HCl polymer (orange), and the GO:TripPEES-CH2NH2:HCl product (purple). A prominent peak is assigned to a new amide C= O bond stretch emerging in the product spectra (green shaded region). The O-H stretch (gray shaded region) shows a slight reduction in the product compared to GO. This is consistent with previous reports on the interactions between primary amine compounds and GO.²⁴ These results suggest that TripPEES-CH2NH2:HCl reacts with GO to produce robust amide linkages.

Pickering Emulsion Formation. To demonstrate how the GO-polymer interaction affects the stability of the Pickering emulsions, oil-in-water emulsions were made. 25 Oil-in-water emulsions refer to oil droplets dispersed in water, whereas a water-in-oil emulsion is water droplets dispersed in oil.²⁶ Pickering emulsions are produced when the oil-water interface is stabilized by solid particles, which in our case is the GO–polymer complex.²⁷ To prepare the oil-in-water emulsion, we first dissolved TripPEES-CH2NH2:HCl polymer in an solution of DMF and ortho-dichlorobenzene (o-DCB), or DMF and chloroform, and then we dispersed this oil phase in a 0.04 wt % GO water dispersion. The oil phase of 0.01 wt % polymer and o-DCB:DMF at a 1:4 ratio yielded stable Pickering emulsions of \sim 5 μ m in diameter (Figure 2B). We obtained a large distribution of emulsion sizes because we used a homogenizer to make the emulsions instead of a microfluidic device, due to the particulate nature of the GO that will clog the latter. Factors that can influence the distribution are the emulsification method, GO concentration, and polymer concentration. 0.01 wt % polymer and DMF:CHCl₃ at a 1:1 ratio as an oil phase were also used to make oil-in-water emulsions, but this produces less stable emulsions than o-DCB emulsions (Figure S7). Larger oil-in-water emulsions were made to observe their interface more closely (Figure S9). There are wrinkles forming at the interface, indicating membrane formation.

Water-in-oil emulsions were also made with a 0.04 wt % GO dispersion as the water phase and a 0.01 wt % polymer solution in chloroform (oil) phase, which yielded stable emulsions of $\sim\!\!20~\mu\mathrm{m}$ in diameter. Emulsions with wrinkled interfacial membranes are observed, which are stable for extended periods (Figure 2C). The formation of stable water-in-oil and oil-inwater emulsions with GO:polymer composites confirm the robust nature of this method. To determine the role that the GO and polymer interaction plays in stabilizing the emulsions, we made control emulsions with the same conditions as above, but without the polymer in the oil phase. The chloroform emulsions were unstable with only GO in the water as the stabilizing agent.

Water Filtration Membranes. Figure 3A schematically illustrates membrane fabrication from oil-in-water emulsions. The emulsions, after the excess GO dispersion is removed,



В

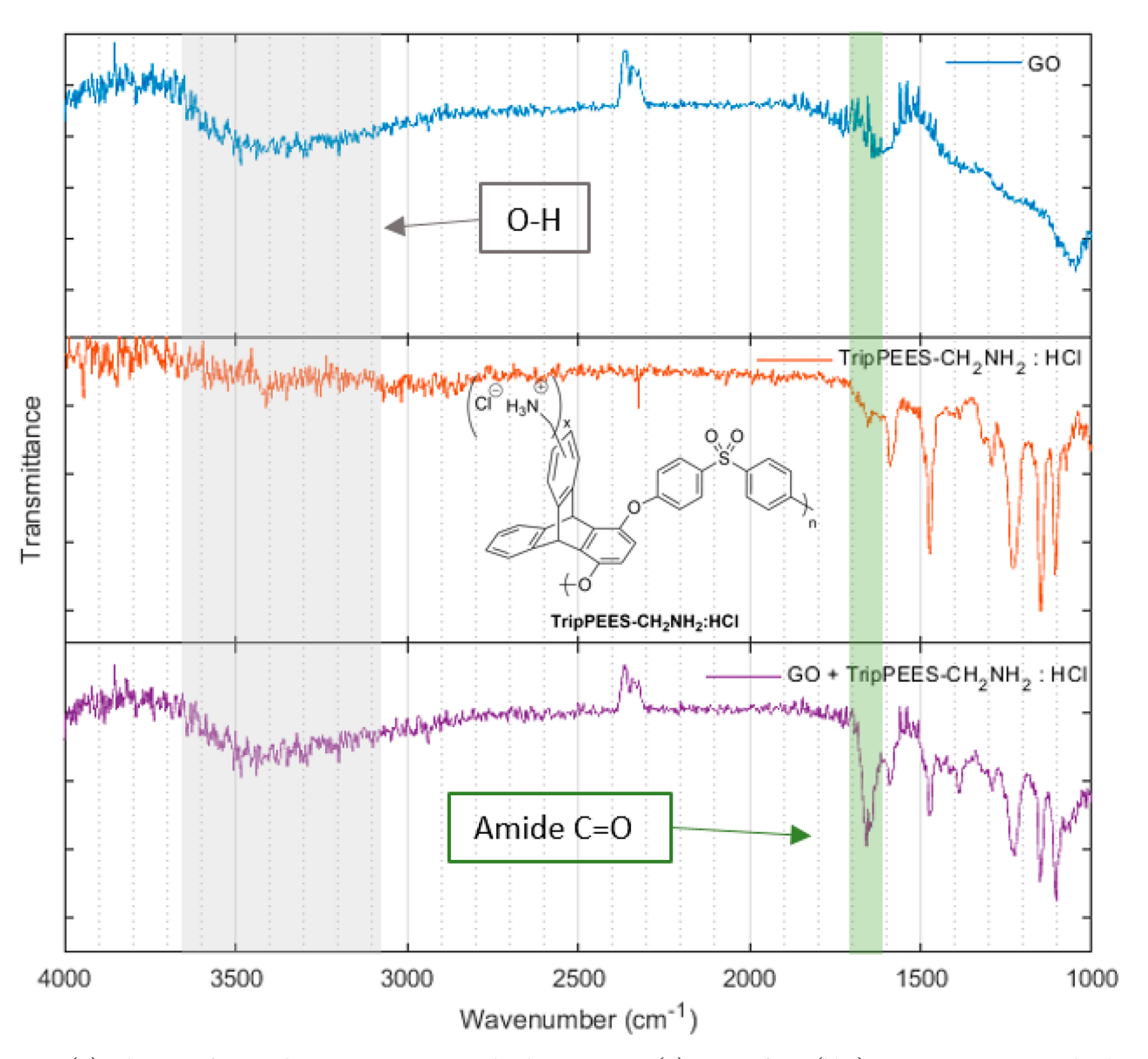


Figure 1. (A) Schematic of GO and TripPEES-CH₂NH₂:HCl polymer reaction, (B) FT-IR of GO (blue), TripPEES-CH₂NH₂:HCl polymer (orange), and TripPEES-CH₂NH₂:HCl polymer and GO (purple).

form a viscous composition which is spread on the polytetrafluoroethylene (PTFE) polymer substrate with a glass pipet. The emulsions are left to dry in the air for up to 3 h wherein they become unstable and coalesce. Our expectation was that the resulting membrane would have the

polymer as the spacer between the GO sheets as a result of the partitioning of the polymer in the particle's interior. Figure 3B shows the optical images of the Pickering emulsion before the top phase of the aqueous GO dispersion is removed. After spreading on the substrate, the emulsion particles are mobile

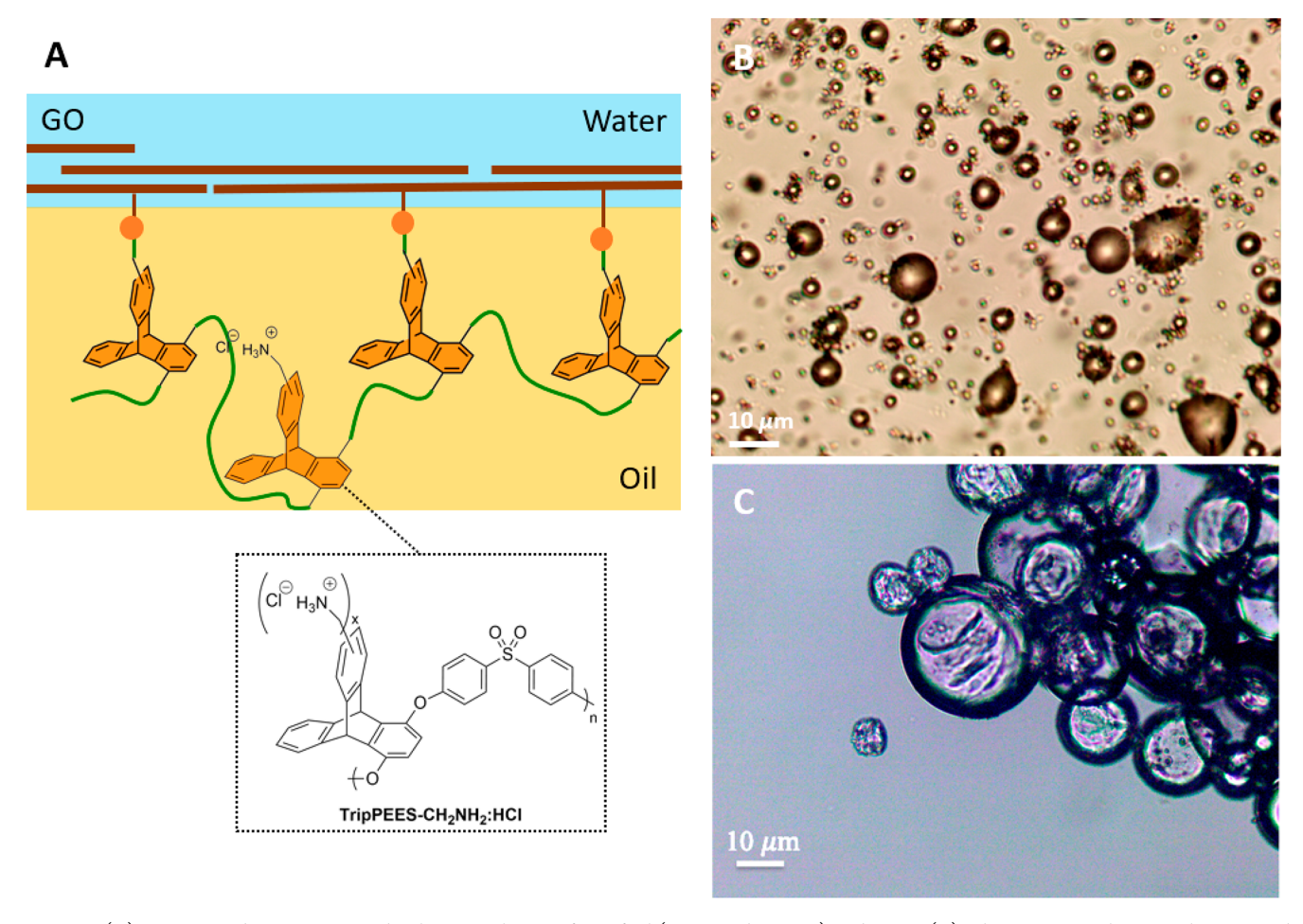


Figure 2. (A) Interaction between GO and polymer at the interface of oil (DMF and o-DCB) and water, (B) oil-in-water emulsions with DMF and o-DCB as the oil phase, and (C) water-in-oil emulsions with chloroform as the oil phase showing membrane formation at the interface.

and assemble into an even surface coating. As the water evaporates, the emulsion particles coalesce and evaporation of the oil phase creates a dried film. After drying, the membrane has a smooth surface and observations with an optical microscope confirm the formation of a continuous film with no sign of the original emulsion structure.

We evaluated the role of the oil composition in the Pickering emulsions and the quality of membrane films. When chloroform was used as the oil phase with DMF as cosolvent, we observed bubbling during the drying process and large round features with examination under the microscope (Figure S8). Chloroform has a lower boiling point than o-DCB, and the bubbles observed are the result of evaporation. We have also noticed that chloroform-containing emulsions also tend to be less stable than those with o-DCB, and they likely burst before coalescence. The problem is mitigated by using a vacuum filtration method to produce the membrane. The application of the vacuum removes liquid chloroform before it vaporizes, which prevents bubbling. To verify that both methods yield the same membrane's composition with the same emulsions, we collected the filtrate from the vacuum filtration and analyzed for any polymer that had passed through the filter. Figure S6 shows that no polymer is detected.

The DMF and o-DCB oil composition was optimized to create a homogeneous and pinhole-free film. Figure 4 shows photographs of fabricating membranes/films wherein the oil composition of o-DCB:DMF ranges from 1:1 to 1:2, 1:3, and

1:4. The polymer substrate is PP-backed PTFE, and with increasing DMF there are fewer cracks and eventually the film is homogeneous at the 1:4 ratio. This is observed for deposition on both hydrophobic and hydrophilic PTFE substrates (Figure S10). A similar trend was observed microscopically as well. In Figures S11 and S12, as we increased the DMF concentration, we observed less and less of the vestiges of the original emulsions. The cracks may form in part as a result of the lack of wettability of the oil solution on the substrate, although we could not confirm this hypothesis with contact angle measurements because of the rapidity at which the emulsion particles spread. However, it has been observed previously that compositions that produce uniform crack-free films are those that best wet the substrate, and increased interfacial tension between the solution and the substrate can produce cracked films. 28,29 To make membranes for water filtration testing, we used emulsions with an oil composition of 1:4 o-DCB:DMF. For the casting method, the solvent evaporation rate is 0.5 mL/h at 21 °C in a wellventilated area.

A key structural feature of any graphene-based membrane is the intersheet spacing that typically manifests a characteristic X-ray diffraction (XRD) peak. Figure 5A (and Figure S13) shows the intersheet spacing in membranes with different polymer concentrations. With increasing polymer concentration, the intersheet spacing increases, which is consistent with our structural model of the GO:polymer composite

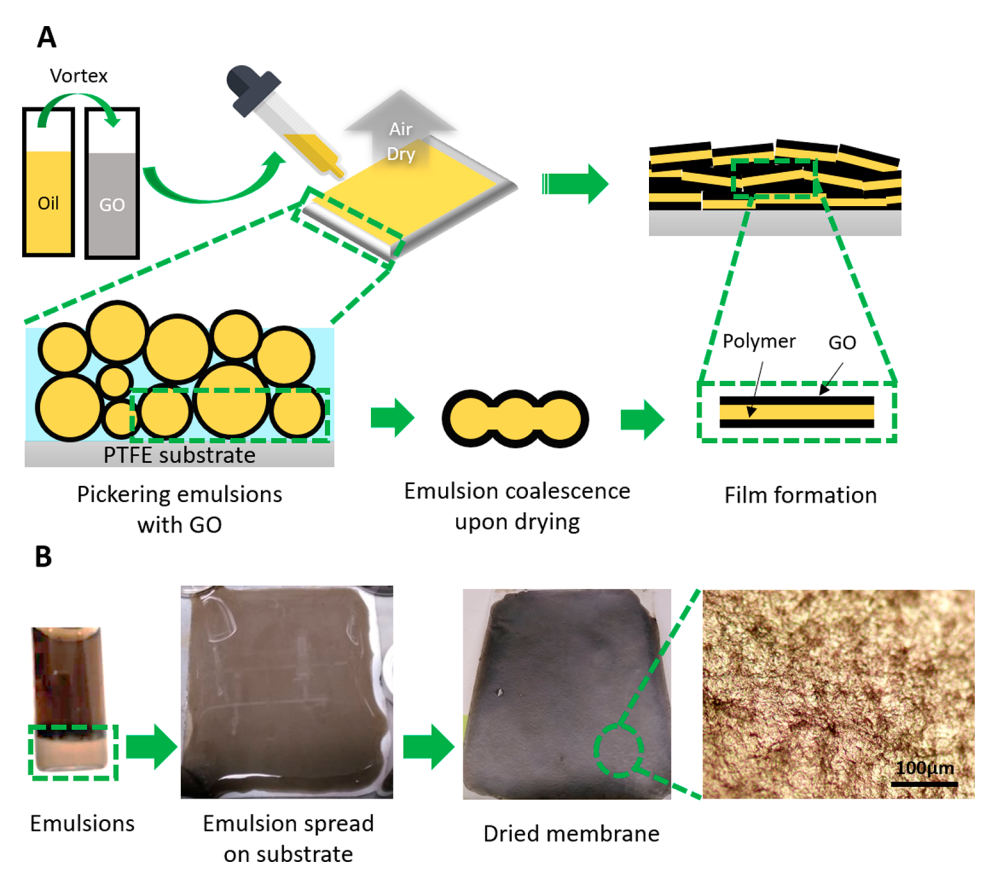


Figure 3. (A) Schematic of membrane fabrication from the oil-in-water emulsion. The oil phase is vortexed into the GO dispersions. The excess GO dispersion is removed, resulting in a viscous emulsion that is spread on the PTFE polymer substrate by a glass pipet. As the water starts to evaporate, the emulsion particles become unstable and coalesce into a continuous film with drying. (B) Images of Pickering emulsions stabilized by GO which was spread on the substrate to dry in the air and a microscopic image showing the surface of the dried film.

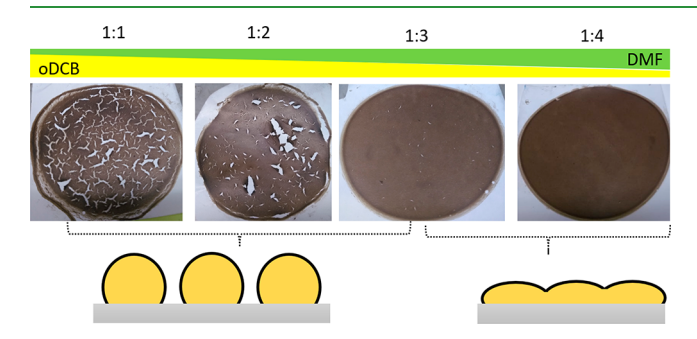


Figure 4. Solvent composition affects the formation of a continuous film. (top) Film morphology with oil composition of varying o-DCB:DMF ratios. (bottom) Schematic demonstrating how a single layer of emulsions wets the surface depending on their oil composition. Multiple layers or stacked layers of emulsions have similar behavior.

membranes,² wherein the polymer behaves as an intersheet spacer. Polymer concentrations in the oil phase above 0.1 wt % result in changes in the membrane's integrity and morphology. Films with the most homogeneous morphology are produced with concentrations less than 0.015 wt %. At higher concentrations, membranes start to show lightly colored spots and can delaminate from the substrate. The polymer is not soluble in water, and as mentioned before, this leads to GO aggregation when the polymer is mixed in a GO dispersion. At higher polymer concentrations, phase separation appears to occur and the light spots are a polymer-rich phase.³⁰

The membrane's thickness was also investigated with varying polymer concentrations. The amount of the emulsions spread over the support was kept constant at 0.126 mL/cm², and the thickness was measured by the scanning electron microscopy (SEM) imaging of a cross-section prepared by freeze-fracturing a membrane. More details and enlarged SEM images are shown in Figure S14. As detailed in Figure 5B, the film thickness increases with increasing polymer concentration. The changes in both the intersheet spacing and thickness confirm that the polymer is fully incorporated into the membrane and acts as a spacer between GO sheets. As the concentration increases from 0 to 0.01 wt %, the thickness increases linearly with the concentration. However, we see a large jump in thickness as we reach 0.015 wt %, which is consistent with the onset of phase separation.

Another observation from Figure 5A,B is that when we added 0.01 wt % polymer to the membrane, the thickness increased more than 100% but the interlayer spacing increased by 10%. The discrepancy is from the phase separation of the polymer and not all polymer is intercalated between the GO sheets. The XRD measurement shows us how much interlayer spacing is changed due to the intercalation of the polymer but does not quantify how much the polymer is phase separated. The film thickness does reveal the additional material that is incorporated into the membrane but does not reveal the thickness increases resulting from polymer intercalation between the GO sheets relative to the polymer-rich phase.

Homogeneous membrane films were evaluated for the water filtration test using a dead-end cell. We initially analyzed a

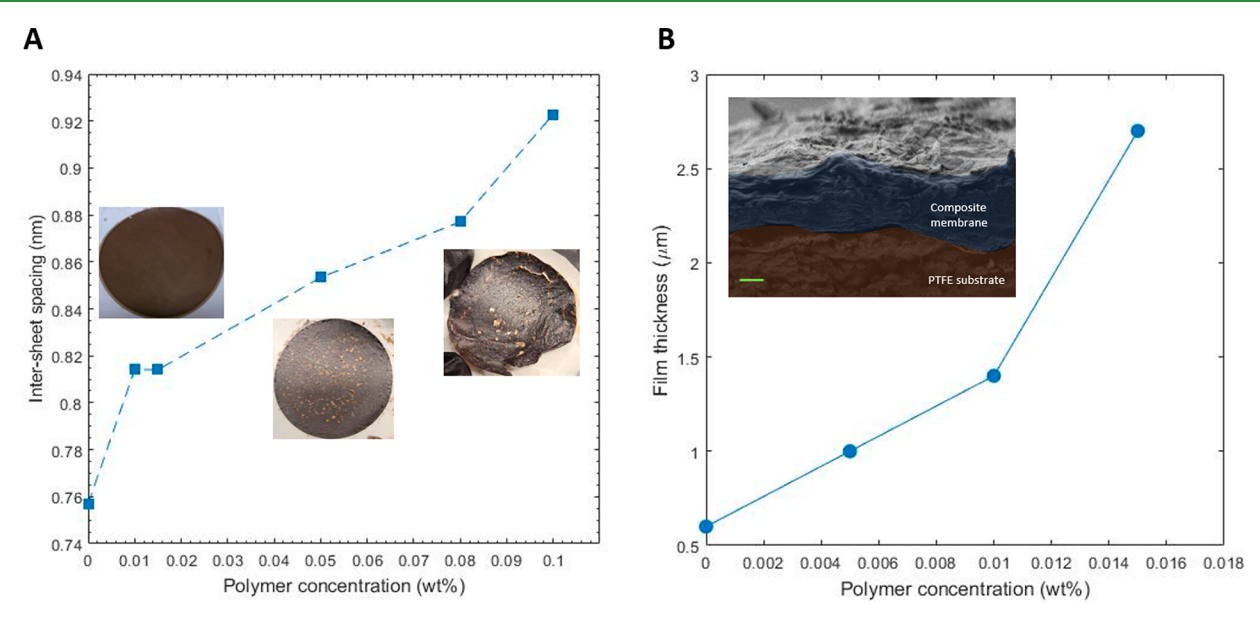


Figure 5. (A) Intersheet spacing of membranes made with different polymer concentration measured by XRD. (B) Film thickness of membranes made with different polymer concentration measured by SEM. The picture shows the cross section of a film made with 0.015 wt %. Scale bar: 1 µm.

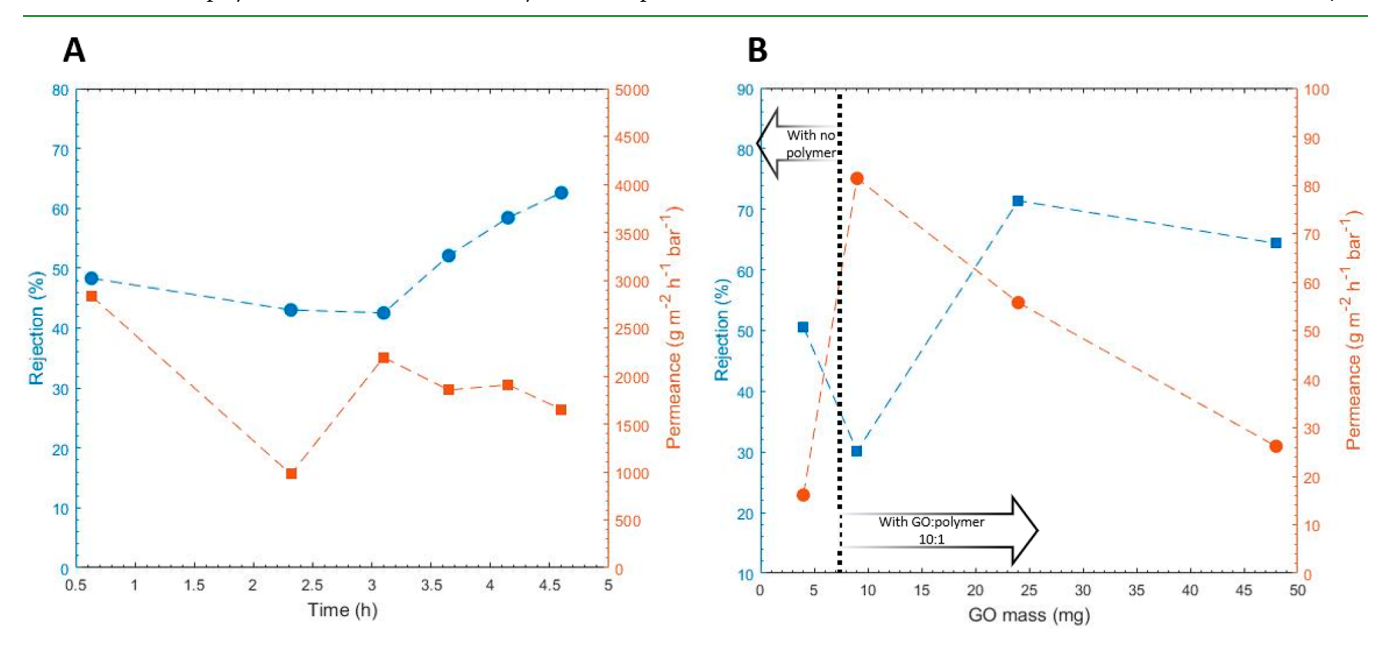


Figure 6. (A) Rejection and permeance of membrane made with 1:4 o-DCB:DMF, 16 mg of GO, and 0.6 mg of polymer on hydrophilic PTFE substrate. (B) Rejection and permeance averages of membranes made with increasing GO loading with and without polymer loading at 10:1 GO:polymer by mass, on a hydrophobic substrate.

solution of 100 ppm Rose Bengal (~1 kDa) at pH 12 to mimic the separation conditions of black liquor from pulp paper manufacturing.³¹ All membranes were made with an emulsion loading of 0.126 mL/cm². Figure 6A shows results from the membrane made with 16 mg GO and 0.6 mg polymer loading (0.01 wt %) on a hydrophilic PTFE substrate. The membrane produced a 65% rejection and 2500 g m⁻² h⁻¹ bar⁻¹, and the permeance decreased over time as a result of material buildup in the membrane.³² Rejection is the percentage of solute removed from the feedwater in a membrane filtration process. It was calculated according to the eq 1 in the Membrane Testing section. The rejection increases steadily throughout the experiment. A polymer concentration higher than 0.01 wt % was used to fabricate thicker membranes. However, the polymer has low solubility in o-DCB, so the increased

concentration of polymer over the course of the emulsion coalescence and drying resulted in a nonuniform membrane. From the performance we displayed from Figure 6A, we can confirm that our method can produce a homogeneous and functional filtration membrane.

We were interested to evaluate how the polymer and graphene oxide loading affects the permeance and rejection characteristics. Figure 6B details the performance of films made with and without the polymer. In the composite membranes, the polymer:GO mass ratio is kept constant at 10:1. We used chloroform and DMF for the oil phase, since the polymer has higher solubility in chloroform. A vacuum filtration setup was used to dry the film instead of air-drying because of chloroform's low boiling point as mentioned earlier. The polymer concentration was held constant at 0.015 wt %, since

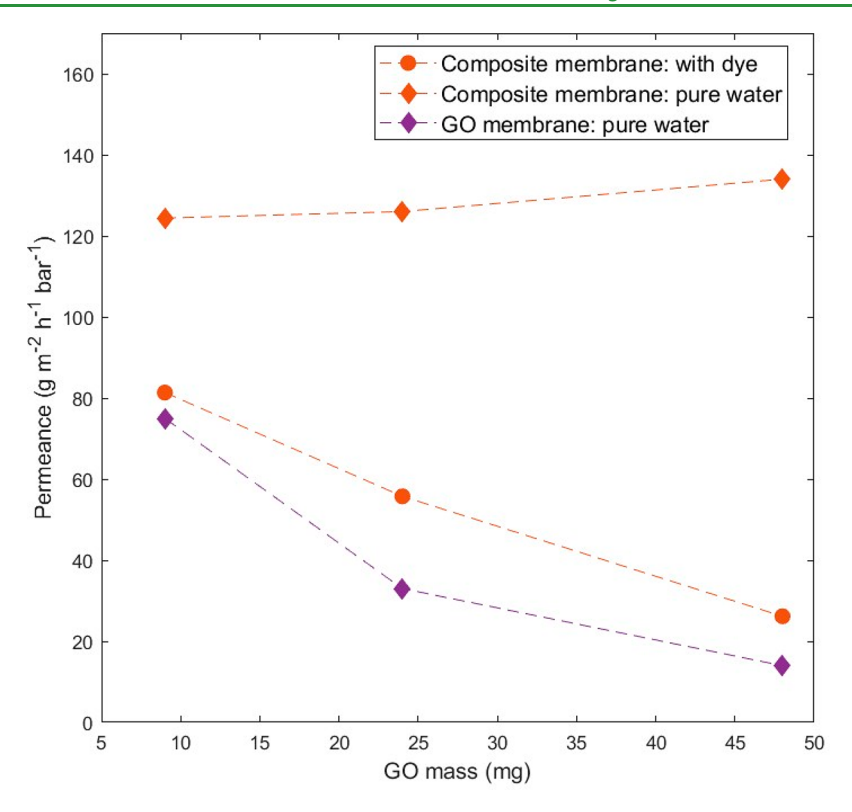


Figure 7. Permeance of composite membranes and GO membranes with dye and pure water. Composite membranes are made with a GO:polymer 10:1 mass ratio. The orange lines denote composite membranes, and the purple line denotes the GO membrane. The circle marker indicates that membranes are tested with pure water, and the diamond marker indicates membranes tested with dye.

we observed that this yields the most consistent morphology with this oil composition. We tested all the membrane compositions in the dead-end setup for up to 7 days. During this period, we did not observe any large change in rejection or permeance (Figure S15). This shows that all of them maintained working conditions during this period. For the composite membranes, the rejection increased from 30% to 70% as the GO and polymer loading increased. Permeance, on the other hand, decreases from 80 to 25 g m⁻² h⁻¹ bar⁻¹ with an increase in GO and polymer loading. Since the polymer concentration is constant for all the composite membranes, the intersheet spacing is invariant in this series. Hence, the trend we observed is the result of the increased thickness of the membrane and increasing layers of GO and polymer.^{33,34}

We observed a large decrease in rejection going from the films without polymer (50%) to films with polymer (30%). There is a significant increase in permeance in transitioning from GO membranes without polymer (15 g m⁻² h⁻¹ bar⁻¹) to composite GO:polymer membranes (85 g m⁻² h⁻¹ bar⁻¹). The performance differences between a pure GO membrane and composite membranes are related to the change in intersheet spacing (Figure 5A) and thickness. In addition, it is likely that the anionic dye, Rose Bengal, adsorbs to our the cationic polymer through electrostatic interactions. As we introduce more polymer, the intersheet spacing increases as well as the diffusion path and dye adsorption capacity of the membrane, which leads to a lower rejection and higher permeance as reported. 34,37

To better understand the composite properties, we measured pure water permeance of the composites and GO membranes. Figure 7 compares the permeances between the composite membrane and GO in dye solution and pure water.

Orange lines show the permeance of composite membranes with the same GO:polymer 10:1 mass ratio. For pure water, the permeance does not show a significant variation with increasing material loading. The addition of dye causes the permeance to decrease gradually. This indicates that the water diffusion through the composite membrane is fast and independent of the thickness of the composite membrane. When the dye is added, permeance decreases by more than 30% because absorption of bulky dye molecules prevents water molecules from diffusing through the membrane. As mentioned, Rose Bengal is an anionic dye that can bind to the cationic polymer in the composite membranes through electrostatic adsorption. This further blocks water diffusion pathways in the membrane, leading to a significant reduction in water permeance.

We compared the permeance of pure water between GO membranes and composite membranes (Figure 7, lines with diamond markers). Figure 7 shows that the more open and porous structure of composite membranes allows the water to diffuse faster in comparison to the GO membranes. GO membranes have a lower permeance when compared to composite membranes. Figure 7 reveals that the porous and open structure of the composite membranes allows water molecules to diffuse through the membrane.

METHODS

Materials. Graphene oxide was purchased from Graphenea in 0.4 wt % 250 mL bottle. Hydrophobic PP-backed PTFE substrates were purchased from Sterlitech, and hydrophilic polypropylene-backed PTFE substrates were purchased from Allpure. The substrate has a pore size of 0.1 μ m. Anhydrous toluene was obtained from an INERT PureSolv MD5 solvent purification system and stored under Ar over 4 Å molecular sieves. Anhydrous solvents including dimethylacetamide

(DMAc) and 1,1,2,2-tetrachloroethane were purchased from Sigma-Aldrich in SureSeal bottles. Anthracene was recrystallized from ethanol/toluene. Benzoquinone was purified by eluting through a plug of silica using CH2Cl2 as the eluent. All other chemicals were purchased from commercial sources and used as received.

Synthesis. Synthesis of TripPEES.

The synthesis of TripPEES was adapted from a previously reported procedure.²³ Anthracene (3.56 g, 20 mmol, 1 equiv), benzoquinone (2.59 g, 24 mmol, 1.2 equiv), and xylenes (20 mL) were refluxed under N2 for 4 h. After cooling to rt, the solids were collected by vacuum filtration and washed with cold toluene and methanol. The product was recrystallized from xylenes (~120 mL) to obtain 9,10dihydro-9,10-[1,2]benzenoanthracene-13,16-dione as a light yellow crystalline solid (4.87 g, 85% yield).

¹H NMR (400 MHz, CDCl₃): δ 7.40 (dd, J = 5.4, 3.3 Hz, 2H), 7.19 (m, 4H), 7.08 (dd, J = 5.4, 3.3 Hz, 2H), 6.31 (s, 2H), 4.87 (s, 2H)2H), 3.14 (s, 2H).

 13 C NMR (101 MHz, CDCl₃): δ 198.5, 141.7, 140.7, 139.8, 126.9, 126.8, 124.9, 124.0, 49.2, 49.1.

HRMS (ESI): calcd for $[M + H]^+ C_{20}H_{15}O_2^+$ 287.1067; found 287.1091.

All glassware was oven-dried. 9,10-Dihydro-9,10-[1,2]benzenoanthracene-13,16-dione (4.8702 g, 17.009 mmol, 1 equiv), bis(4-fluorophenyl)sulfone (4.3245 g, 17.009 mmol, 1 equiv), and K₂CO₃ (5.40 g, 39.1 mmol, 2.3 equiv) were placed in a two-neck flask and purged with Ar. The flask was fitted with a short-path distillation apparatus. Anhydrous DMAc (50 mL) and toluene (12 mL) were added. The mixture was heated at 150 °C for 6 h, during which the toluene and water formed from K2CO3 were azeotropically distilled off. Afterward, the distillation apparatus was replaced with a reflux condenser, and the mixture was refluxed at 180 °C for 18 h. The mixture was precipitated in warm water, and the solids were collected by vacuum filtration, washed with water, and dried in a vacuum oven at 60 °C. The dried polymer was redissolved in DMAc and precipitated in warm water again, and the solids were collected by vacuum filtration, washed with water, and dried in a vacuum oven at 60 °C. The dried polymer was dissolved in chloroform and precipitated in methanol, and the solids were collected by vacuum filtration, washed with methanol, and dried in a vacuum oven to obtain an off-white solid (7.75 g, 91% yield).

¹H NMR (400 MHz, CDCl₃): δ 7.89 (d, I = 8.6 Hz, 4H), 7.02 (m, 4H), 6.91 (m, 8H), 6.67 (s, 2H), 5.41 (s, 2H).

SEC: $M_n = 56 \text{ kDa}$, D = 2.06.

Chloromethylation of TripPEES to Obtain TripPEES-CH2Cl.

The chloromethylation of TripPEES was performed following a previously reported procedure.³⁸ TripPEES (1.50 g, 3.0 mmol, 1 equiv of repeating units) was dissolved in anhydrous 1,1,2,2-tetrachloroethane (50 mL) under Ar. Chloromethyl methyl ether (6.84 mL, 90 mmol, 30 equiv) was added, followed by ZnCl₂ (1.23 g, 9 mmol, 3 equiv) under an Ar flow. The mixture was stirred at 60 °C for 5.5 h for a functionalization density (x) of 1.2 (x) can be tuned by the reaction time). After the reaction, the polymer solution was precipitated in methanol, and the precipitate was collected by vacuum filtration and washed thoroughly with methanol, water, and then methanol again. The polymer was dried under vacuum to give an offwhite solid (90-95% yields typically obtained). The level of functionalization (x) was determined using the NMR integration ratios of the ArCH2Cl protons and the bridgehead CH protons.

¹H NMR (400 MHz, CDCl₃): δ 7.90 (m, 4H), 6.92 (m, \sim 11H), 6.69 (br s, 2H), 5.42 (m, 2H), 4.37 (m, 2.4H) (for x = 1.2; integration values vary based on x).

Gabriel Amine Synthesis to Obtain TripPEES-CH2NH2.

TripPEES-CH₂Cl (1.54 g, α = 1.2, 2.75 mmol of polymer backbone repeating units, 3.3 mmol of benzyl chloride groups) was dissolved in anhydrous DMAc (60 mL) under Ar. Potassium phthalimide (1.83 g, 9.9 mmol, 3 equiv vs benzyl chloride) and NaI (49 mg, 0.33 mmol, 0.1 equiv vs benzyl chloride) were added under Ar flow. The mixture was stirred at 45 °C for 18 h. After the reaction, the mixture was precipitated in 10:1 water/methanol, and the precipitate was collected by vacuum filtration, washed with water and methanol, and dried under vacuum to give TripPEES-CH2phthalimide as a white solid that was used directly for the next step.

TripPEES-CH₂phthalimide was dissolved in dioxane (50 mL). To the polymer solution was added a solution of hydrazine monohydrate (2.4 mL, 50 mmol, 15 equiv vs benzyl chloride) in dioxane (5 mL). The mixture was heated at 90 °C for 18 h, during which it became a white dispersion. After the reaction, the mixture was precipitated in 10:1 0.1 M NaOH/methanol, and the precipitate was collected by vacuum filtration to give TripPEES-CH2NH2 as a white solid (1.32 g, 92% yield over two steps). The product was stored in the freezer to impede gradual cross-linking

¹H NMR (400 MHz, CDCl₃): δ 7.89 (m 4H), 6.92 (m, \sim 11H), 6.67 (br s, 2H), 5.40 (m, 2H), 3.64 (m, 1.5H) (for x = 0.75; integration values vary based on x).

Preparation of HCl Salt of TripPEES-CH₂NH₂.

367 mg of TripPEES-CH2NH2 was dissolved in ~7 mL of DMF, and 1.6 mL of 1 M HCl (~2 equiv relative to amines) was added dropwise with stirring. The solution was then dialyzed against water and lyophilized to give a slightly brown fluffy solid.

Emulsion Preparation. Oil-in-water emulsions were made with 0.04 wt % GO as the water phase. The oil phase was a solution of o-DCB and DMF in volume ratios of 1:1, 1:2, 1:3, and 1:4 or a solution of DMF and chloroform in a volume ratio of 1:1. The polymer was dissolved in DMF at different weight concentrations. To make the dispersions, 8 mL of oil was added to 40 mL of 0.04 wt % GO. Homogenizer (Tissue Tearor Model 985370) was used to mix the two phases.

Membrane Fabrication. The emulsion was left to settle for 10 min. Most of the particles fell to the bottom of the water solution. The excess water phase was removed, which created a viscous paste. This was spread onto the substrate with a pipet and left to dry in air.

Membrane Testing. Dead-end cells (HP4750) were purchased from Sterlitech. 250 mL of a 0.01 M NaOH solution (pH = 12) and a 100 ppm Rose Bengal solution were poured slowly into the cell to prevent breakage of the membrane due to fast water flow. Nitrogen gas with a pressure of 75 psi was used. The permeate was collected in a 20 mL vial. To calculate the permeance, the weight of permeate was measured and the collection time was recorded. The active area was $19.6~{\rm cm}^2$. The rejection was calculated by eqs 1-3

rejection(n) =
$$100 - \frac{I_{p(n)}}{I_{r(n-1)}} \times 100\%$$
 (1)

$$I_{r(n-1)} = \frac{I_{r(n-2)} \times V_{r(n-2)} - I_{p(n-1)} \times V_{p(n-1)}}{V_{r(n-2)} - V_{p(n-1)}}$$
(2)

$$I_{\mathbf{r}(o)} = I_{\mathbf{f}} \quad V_{\mathbf{r}(o)} = V_{\mathbf{f}} \tag{3}$$

where I is the UV—vis absorbance at \sim 548 nm, the conductivity, or the refractive index, V is the volume, n is the sample number, p is the permeate, p is the remainder, and p is the feed.

CONCLUSION

In summary, GO-stabilized Pickering emulsions enable a simple method to fabricate GO/polymer composite water filtration membranes. The cross-linking between synthesized TripPEES-CH2NH2:HCl and GO results in the formation of stable Pickering emulsions under a variety of conditions (water-in-oil, oil-in-water). The casting of emulsions and drying on supports resulted in the coalescence of particles to create membranes with smooth and homogeneous morphologies. To produce crack-free membranes, oil compositions showing good wettability on the substrate (PP-backed PTFE) were selected. The intersheet spacing of the GO and the thickness of the composite membrane can be controlled by varying the amount of polymer in the emulsion, and as confirmed by XRD and SEM, the polymer acts as the spacer between GO sheets. The composite membrane was used to filter a Rose Bengal solution and achieved a 65% rejection and a 2500 g m⁻² h⁻¹ bar⁻¹ flux across the membrane. Composite membranes with low GO and polymer loading have lower rejection and higher permeability than GO membranes as a result of the increase in intersheet spacing. With higher GO and polymer loading, a thicker composite membrane outperforms the GO membrane. We find that at all film thicknesses, composites show higher water permeance compared to the GO membrane. Hence, polymer incorporation improved the performance of the GO membranes. This method for membrane manufacturing is general and scalable and can be used to produce other membranes and coatings.

ASSOCIATED CONTENT

Supporting Information

The Supporting Information is available free of charge at https://pubs.acs.org/doi/10.1021/acsami.3c02636.

NMR characterization, optical microscopy data, film coating data, XRD characterization data, SEM characterization data, membrane stability study, and instrumentation (PDF)

AUTHOR INFORMATION

Corresponding Author

Timothy M. Swager — Department of Chemistry, Massachusetts Institute of Technology, Cambridge, Massachusetts 02139, United States; oocid.org/0000-0002-3577-0510; Email: tswager@mit.edu

Authors

Quynh P. Ngo – Department of Chemistry, Massachusetts Institute of Technology, Cambridge, Massachusetts 02139, United States; Department of Materials Science and Engineering, Massachusetts Institute of Technology, Cambridge, Massachusetts 02139, United States;
oorcid.org/0000-0002-9463-3356

Weize Yuan — Department of Chemistry, Massachusetts Institute of Technology, Cambridge, Massachusetts 02139, United States; orcid.org/0000-0001-9240-507X

You-Chi Mason Wu — Department of Chemistry, Massachusetts Institute of Technology, Cambridge, Massachusetts 02139, United States; ⊚ orcid.org/0000-0002-6585-7908

Complete contact information is available at: https://pubs.acs.org/10.1021/acsami.3c02636

Notes

The authors declare no competing financial interest.

ACKNOWLEDGMENTS

This work was supported by the National Science Foundation (DMR-1809740 and DMR-2207299). The authors gratefully acknowledge Via Separations for funding this research through an ARPA-E Award (DE-AR0001043). We thank Dr. Michelle Chen and Dr. Hari Vijayamohanan in the Swager group for insightful discussions and suggestions.

REFERENCES

- (1) Sholl, D. S.; Lively, R. P. Seven Chemical Separations to Change the World. *Nat.* 2016 5327600 **2016**, 532, 435–437.
- (2) Xue, S.; et al. Nanostructured Graphene Oxide Composite Membranes with Ultrapermeability and Mechanical Robustness. *Nano Lett.* **2020**, *20*, 2209–2218.
- (3) Smith, A. T.; LaChance, A. M.; Zeng, S.; Liu, B.; Sun, L. Synthesis, Properties, and Applications of Graphene Oxide/Reduced Graphene Oxide and Their Nanocomposites. *Nano Mater. Sci.* **2019**, *1*, 31–47.
- (4) Dong, Y.; et al. Single-Layered GO/LDH Hybrid Nanoporous Membranes with Improved Stability for Salt and Organic Molecules Rejection. *J. Membr. Sci.* **2020**, *607*, 118184.
- (5) Abdelkader, B. A.; Antar, M. A.; Laoui, T.; Khan, Z. Development of Graphene Oxide-Based Membrane as a Pretreatment for Thermal Seawater Desalination. *Desalination* **2019**, 465, 13–24.
- (6) Liu, H.; et al. Thermo- and pH-Responsive Graphene Oxide Membranes with Tunable Nanochannels for Water Gating and Permeability of Small Molecules. *J. Membr. Sci.* **2019**, *587*, 117163.
- (7) Kang, H.; et al. Sandwich Morphology and Superior Dye-Removal Performances for Nanofiltration Membranes Self-Sssemblied Via Graphene Oxide and Carbon Nanotubes. *Appl. Surf. Sci.* **2018**, 428, 990–999.
- (8) Han, Z.; et al. A Review of Performance Improvement Strategies for Graphene Oxide-Based and Graphene-Based Membranes in Water Treatment. *J. Mater. Sci.* **2021**, *56*, 9545–9574.
- (9) Akbari, A.; et al. Large-Area Graphene-Based Nanofiltration Membranes by Shear Alignment of Discotic Nematic Liquid Crystals of Graphene Oxide. *Nat. Commun.* **2016**, *7*, 10891.
- (10) Kim, H. W.; et al. Selective Gas Transport Through Few-Layered Graphene and Graphene Oxide Membranes. *Science* (80-.). **2013**, 342, 91–95.
- (11) Zhu, Y.; et al. Graphene and Graphene Oxide: Synthesis, Properties, and Applications. Adv. Mater. 2010, 22, 3906–3924.
- (12) Decher, G. Fuzzy nanoassemblies: Toward Layered Polymeric Multicomposites. *Science* (80-.). **1997**, 277, 1232–1237.
- (13) Suter, J. L.; et al. Principles Governing Control of Aggregation and Dispersion of Graphene and Graphene Oxide in Polymer Melts. *Adv. Mater.* **2020**, *32*, 2003213.
- (14) Sydlik, S. A.; Swager, T. M. Functional Graphenic Materials Via a Johnson-Claisen Rearrangement. *Adv. Funct. Mater.* **2013**, 23, 1873–1882.

- (15) Ngo, Q. P.; et al. Reconfigurable Pickering Emulsions with Functionalized Carbon Nanotubes. *Langmuir* **2021**, *37*, 8204–8211.
- (16) Qian, Y.; et al. Enhanced Ion Sieving of Graphene Oxide Membranes via Surface Amine Functionalization. *J. Am. Chem. Soc.* **2021**, *143*, 5080–5090.
- (17) Stankovich, S.; et al. Systematic Post-Assembly Modification of Graphene Oxide Paper with Primary Alkylamines. *Chem. Mater.* **2010**, 22, 4153–4157.
- (18) Hosseini, Y.; Najafi, M.; Khalili, S.; Jahanshahi, M.; Peyravi, M. Assembly of Amine-Functionalized Graphene Oxide for Efficient and Selective Adsorption of CO2. *Mater. Chem. Phys.* **2021**, *270*, 124788.
- (19) Kim, S.; et al. An Aggregation-Mediated Assembly of Graphene Oxide on Amine-Functionalized Poly(Glycidyl Methacrylate) Microspheres for Core-Shell Structures with Controlled Electrical Conductivity. *J. Mater. Chem. C* **2014**, *2*, 6462–6466.
- (20) Gu, M. J.; Wang, Y. F.; Han, Y.; Chen, C. F. Recent Advances on Triptycene Derivatives in Supramolecular and Materials Chemistry. *Org. Biomol. Chem.* **2021**, *19*, 10047–10067.
- (21) Aizawa, T.; Wakui, Y. Correlation Between the Porosity and Permeability of a Polymer Filter Fabricated via CO2-Assisted Polymer Compression. *Membranes (Basel)*. **2020**, *10*, 391.
- (22) Zhang, N.; et al. Mechanically Reinforced Phosphoric Acid Doped Quaternized Poly(Ether Ether Ketone) Membranes via Cross-Linking with Functionalized Graphene Oxide. *Chem. Commun.* **2014**, 50, 15381–15384.
- (23) Kim, Y.; Moh, L. C. H.; Swager, T. M. Anion Exchange Membranes: Enhancement by Addition of Unfunctionalized Triptycene Poly(Ether Sulfone)s. *ACS Appl. Mater. Interfaces* **2017**, *9*, 42409–42414.
- (24) Chen, L.; Huang, L.; Zhu, J. Stitching Graphene Oxide Sheets into a Membrane at a Liquid/Liquid Interface. *Chem. Commun.* **2014**, 50, 15944–15947.
- (25) Guo, P.; Song, H.; Chen, X. Hollow Graphene Gxide Spheres Self-Assembled by W/O Emulsion. *J. Mater. Chem.* **2010**, 20, 4867–4874.
- (26) Oil-in-Water Emulsions. https://www.hielscher.com/oil-in-water-emulsions.htm. Accessed 20 August 2022.
- (27) Yang, Y.; et al. An Overview of Pickering Emulsions: Solid-Particle Materials, Classification, Morphology, and Applications. *Front. Pharmacol.* **2017**, *8*, 287.
- (28) Dukarov, S.; Kryshtal, A.; Sukhov, V. Surface Energy and Wetting in Island Films In Wetting and Wettability; InTech: 2015. DOI: 10.5772/60900
- (29) Bonn, D. Wetting Transitions. Curr. Opin. Colloid Interface Sci. **2001**, 6, 22–27.
- (30) Sandoval, S.; Fuertes, A.; Tobias, G. Solvent-Free Functionalisation of Graphene Oxide with Amide and Amine Groups at Room Temperature. *Chem. Commun.* **2019**, *55*, 12196–12199.
- (31) Introduction To Liquor Of Paper Pulping | Black Liquor, White Liquor. http://www.paperpulpingmachine.com/introduction-to-liquor-of-paper-pulping/. Accessed 20 August 2022.
- (32) Makogon, T. Y. Flow Restrictions and Blockages in Operations. *Handb. Multiph. Flow Assur.* **2019**, 95–189.
- (33) Yoo, B. M.; Shin, J. E.; Lee, H. D.; Park, H. B. Graphene and Graphene Oxide Membranes for Gas Separation Applications. *Curr. Opin. Chem. Eng.* **2017**, *16*, 39–47.
- (34) Hung, W. S.; et al. Cross-Linking with Diamine Monomers to Prepare Composite Graphene Oxide-Framework Membranes with Varying D-Spacing. *Chem. Mater.* **2014**, *26*, 2983–2990.
- (35) Jia, F.; et al. Advances in Graphene Oxide Membranes for Water Treatment. *Nano Res.* 2022 157 2022, 15, 6636–6654.
- (36) Argüeso, P.; Tisdale, A.; Spurr-Michaud, S.; Sumiyoshi, M.; Gipson, I. K. Mucin Characteristics of Human Corneal-Limbal Epithelial Cells that Exclude the Rose Bengal Anionic Dye. *Invest. Ophthalmol. Vis. Sci.* **2006**, 47, 113.
- (37) Feng, X.; Huang, R. Y. M. Liquid Separation by Membrane Pervaporation: A Review. *Ind. Eng. Chem. Res.* **1997**, *36*, 1048–1066.

(38) Zhao, Z.; Gong, F.; Zhang, S.; Li, S. Poly(Arylene Ether Sulfone)s Ionomers Containing Quaternized Triptycene Groups for Alkaline Fuel Cell. *J. Power Sources* **2012**, *218*, 368–374.

□ Recommended by ACS

Polymer-Grafted Graphene Oxide as a High-Performance Nanofiller for Modification of Forward Osmosis Membrane Substrates

Seyed Reza Razavi, Hossein Mahdavi, et al.

NOVEMBER 23, 2022

ACS APPLIED POLYMER MATERIALS

READ 🗹

Polymer-Grafted Graphene Oxide/Polybenzimidazole Nanocomposites for Efficient Proton-Conducting Membranes

Anupam Das, Tushar Jana, et al.

APRIL 03, 2023

ACS APPLIED NANO MATERIALS

READ 🗹

Exploration of Permeation Resistance Change of the Polyamide Nanofiltration Membrane during Heat Curing by Using Organic Molecules as Functional Fillers

Liu-Kun Wu, Yong-Jian Tang, et al.

OCTOBER 20, 2022

INDUSTRIAL & ENGINEERING CHEMISTRY RESEARCH

READ 🗹

Development of Performance-Enhanced Graphene Oxide-Based Nanostructured Thin-Film Composite Seawater Reverse Osmosis Membranes

Rutuja Bhoje, Parag R. Nemade, et al.

FEBRUARY 09, 2022

ACS APPLIED POLYMER MATERIALS

READ 🗹

Get More Suggestions >